

Mixing and Ergodicity in Systems with Long-Range Interactions

Tarcísio N. Teles,¹ Renato Pakter,² and Yan Levin^{2,*}

¹*Grupo de Física de Feixes, Universidade Federal de Ciências da Saúde de Porto Alegre (UFCSPA), Porto Alegre, RS, Brazil*

²*Instituto de Física, Universidade Federal do Rio Grande do Sul (UFRGS), Porto Alegre, RS, Brazil*

(Dated: January 28, 2025)

We present a theory of collisionless relaxation in systems with long-range interactions. Contrary to Lynden-Bell's theory of violent relaxation, which assumes global ergodicity and mixing, we show that quasi-stationary states (qSS) observed in these systems exhibit broken global ergodicity. We propose that relaxation towards equilibrium occurs through a process of local mixing, where particles spread over energy shells defined by the manifold to which their trajectories are confined. To demonstrate our theory, we study the Hamiltonian Mean Field (HMF) model, a paradigmatic system with long-range interactions. Our theory accurately predicts the particle distribution functions in qSS observed in molecular dynamics simulations without any adjustable parameters. Additionally, it precisely forecasts the phase transitions observed in the HMF model.

PACS numbers: 05.20.-y, 05.70.Ln, 05.70.Fh

Since the pioneering works of Clausius, Boltzmann, and Gibbs, it has been established that systems with short-range (SR) forces reach thermodynamic equilibrium [1]. However, systems with long-range (LR) interactions, where pair potentials decay by a power law with an exponent equal to or less than the spatial dimensionality, are more complex [2]. LR interactions make these systems intrinsically non-extensive, though extensivity can be recovered via the Kac prescription [3], which scales the interaction potential with the number of particles. Even in this "mean-field" limit, LR systems remain non-additive, exhibiting phenomena like ensemble inequivalence, negative specific heat, and temperature jumps in the microcanonical ensemble [4–7].

From a dynamical perspective, LR systems are characterized by diverging collision times, which can exceed astronomical timescales, as seen in elliptical galaxies [8]. In the limit of a large number of particles, these systems do not reach thermodynamic equilibrium but instead become trapped in non-equilibrium quasi-stationary states (qSS), whose lifetime diverges with the system size [9, 10]. The ubiquity of qSS in systems ranging from globular clusters to cold atom setups [11–15] underscores the importance of studying collisionless relaxation.

For systems with SR interactions, the state of thermodynamic equilibrium is unique – it is independent of the initial particle distribution, and only depends on the conserved quantities. On the other hand qSS to which systems with LR interactions evolve depends explicitly on the initial particle distribution. The evolution of the one-particle distribution function $f(\vec{r}, \vec{p}, t)$ is governed by the Vlasov equation, analogous to the dynamics of an incompressible fluid in a six dimensional phase space [16]. However, solving this equation numerically poses significant challenges, leading most studies of LR systems to rely on Molecular Dynamics (MD) simulations.

A number of statistical theories attempting to explain the nature of qSS have been proposed over the years. In

a pioneering work Lynden-Bell (LB) proposed that there is ergodicity and global mixing of the density levels of the initial distribution function during the dynamical evolution of the system [17]. Under these assumptions the final qSS corresponds to the state that maximizes Boltzmann entropy subject to the conservation of the Casimir invariants of the Vlasov dynamics [18]. The resulting distribution functions obtained using such approach, however, were found to deviate significantly from the results of MD simulations, even for the simplest one-level water-bag initial distribution [19–24].

A different approach introduced in 2008 posits that LR systems relax to a core-halo (CH) distribution with a fully degenerate core [11]. Such distributions arise when "wave-particle" interactions and Landau damping govern the system's evolution [2]. Numerical observations of core-halo structures trace back to early simulations by Lecar and Feix of self-gravitating one-dimensional systems [25, 26]. The boundary of the halo region can be understood through the dynamics of test particles interacting with an oscillating mean-field potential [27]. The parametric resonances responsible for energy gain in some particles also lead to evaporative cooling of the core. The CH theory suggests that evaporation ceases when all low-energy states in the core are occupied. For an initial water-bag particle distribution, the CH theory predicts the resulting qSS across a wide range of systems [2]. However, both LB and CH theories have recently been shown to fail with more complex continuous initial distributions, particularly when initial particle distributions exhibit population inversion—where high-energy states have more particles than low-energy states [28], as illustrated in Fig. 1. Under such conditions, the final qSS neither aligns with LB theory predictions nor reflects the fully degenerate core suggested by CH theory.

In this Letter, we will present a new theory that is able to quantitatively predict the results of MD simulations for arbitrary initial conditions without any adjustable pa-

rameters. To explain the new theory we will consider the paradigmatic model of a system with long-range interactions the, so called, Hamiltonian Mean Field (HMF) model. HMF can be considered a dynamical version of the classic XY spin chain, or as N particles moving on a ring, the dynamics of which is governed by the Hamiltonian

$$H = \sum_{k=1}^N \frac{p_k^2}{2} + \frac{1}{2N} \sum_{k,j=1}^N [1 - \cos(\theta_k - \theta_j)], \quad (1)$$

where $\theta_k \in [-\pi, \pi)$ denotes the canonical position coordinate of a particle k , and p_k is its conjugate momentum [29]. Note that all the particles interact with each other. The model also corresponds to the lowest order approximation of a periodic 1d gravity with a “neutralizing” antimatter background [11]. The Kac $1/N$ prefactor is included to make the energy extensive [3]. The particle dynamics is governed by the Hamilton equations of motion:

$$\begin{cases} \dot{\theta}_k = p_k, \\ \dot{p}_k = -m_x(t) \sin \theta_k + m_y(t) \cos \theta_k, \end{cases} \quad (2)$$

where m_x and m_y represent the components of the magnetization vector $\vec{m}(t) = (m_x(t), m_y(t)) = \frac{1}{N} \sum_{k=1}^N (\cos \theta_k, \sin \theta_k)$. To simplify the presentation, we will focus on symmetric distributions for which $m_y(t) = 0$ throughout the evolution. Therefore, the dynamics is fully characterized by $m_x(t)$, which for brevity we shall denote as $m(t)$. The system’s dynamics conserves the total energy, $U = N\langle \varepsilon \rangle / 2 - N(1 - m^2) / 2$, where $\varepsilon(\theta, p, t) = \frac{p^2}{2} + 1 - m(t) \cos \theta$ represents the single particle energy and $\langle \cdot \rangle$ represents the average over the phase space.

Suppose that initially particles are distributed according to

$$f_0(\theta, p) = \frac{2}{\pi p_0 \theta_0} \left(\frac{\theta^2}{\theta_0^2} + \frac{p^2}{p_0^2} \right) \Theta \left[1 - \left(\frac{\theta^2}{\theta_0^2} + \frac{p^2}{p_0^2} \right) \right], \quad (3)$$

where Θ is the Heaviside step function. This distribution exhibits population inversion and the initial energy u_0 and initial magnetization m_0 per particle can be varied by changing the values of θ_0 and p_0 . Since this distribution is not a stationary solution of the Vlasov equation, the dynamics of particles will follow Eqs. 2, eventually evolving to the final qSS shown in Figure 1. Clearly, the particle distribution in the qSS is very different from the predictions of LB (blue dot dashed curves) and CH theories (red dashed curves). On the other hand, the solid curves show the results of the theory that will be presented in this Letter. As can be seen, it captures very well the structure of the qSS, without any adjustable parameters.

The failure of LB theory to correctly account for the particle distribution in the qSS can be traced to the

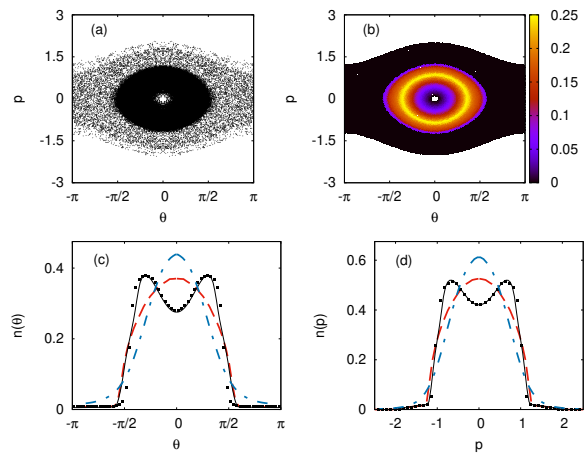


FIG. 1. Panel (a) shows a snapshot of the particle distribution in the qSS obtained from molecular dynamics (MD) simulations with $N = 10^5$ particles. Panel (b) presents the distribution function calculated using the theory to be presented here, with the color scale representing its values. Panel (c) depicts the marginal particle distribution in angle, while panel (d) shows the marginal distribution in momentum compared to MD simulations (symbols). The initial distribution, given by Eq. (3), has $m_0 = 0.475$ and $u_0 = 0.5$, with the qSS magnetization at $m_{qSS} = 0.63$. The dot-dashed blue curves represent predictions from LB theory, calculated using the Monte Carlo simulation method described in reference [28], while the dashed red curves correspond to predictions from CH theory [30]. The black solid curves represent the predictions of the theory presented in this letter.

breakdown of the key assumption of ergodicity and global mixing on which the theory is based. On the other hand, it is natural to expect that the nonlinearity of dynamics will lead to phase mixing of particles along the trajectories of fixed energy. We shall, therefore, proceed to relax the LB assumption of global ergodicity, to a much less restrictive assumption of local mixing along the isoenergy trajectories defined by the single-particle energy a similar idea was introduced at 2009 to study a set of uncoupled pendula [31].

The assumption of local mixing means that for a fixed initial magnetization m_0 , particle from the initial distribution $f_0(\theta, p)$ that have the same energy ϵ will mix uniformly over the isoenergy trajectories resulting in a coarse-grained particle distribution given by:

$$\bar{f}_0(\epsilon) = \frac{\iint d\theta dp f_0(\theta, p) \delta[\varepsilon_0(\theta, p; 0) - \epsilon]}{\iint d\theta dp \delta[\varepsilon_0(\theta, p; 0) - \epsilon]}, \quad (4)$$

The numerator of Eq. (4) corresponds to the number of particles in $f_0(\theta, p)$ with energies in the interval $[\epsilon; \epsilon + d\epsilon]$, while the denominator to the phase space volume corresponding to this energy interval.

The integrals in momentum in Eq. 4 can be evaluated using the well known property of the Dirac delta function $\delta[h(z)] = \sum_j \frac{\delta(z - z_j)}{|h'(z_j)|}$, where z_j is the j -th root of $h(z)$.

Furthermore, the integral over θ in the denominator can be performed explicitly in terms of elliptic integral functions, resulting in:

$$\bar{f}_0(\epsilon) = \frac{\int d\theta \frac{f_0[\theta, \sqrt{2(\epsilon-1+m_0 \cos \theta)}]}{\sqrt{2(\epsilon-1+m_0 \cos \theta)}}}{g_0(\epsilon)}, \quad (5)$$

where,

$$g_0(\epsilon) = \begin{cases} 2\sqrt{|m_0|}K(\kappa_0) & \text{if } \kappa_0 \leq 1 \\ 2K(\kappa_0^{-1})/\sqrt{(|m_0|\kappa_0)} & \text{if } \kappa_0 > 1 \end{cases} \quad (6)$$

with $\kappa_0 = (\epsilon_0 - 1 + |m_0|)/(2|m_0|)$ and $K(x)$ is the complete elliptic integral of the first kind. If the initial state is such that the magnetization remains constant after the mixing process, the distribution given by Eq. 5 will correspond to the qSS (quasi-stationary state) attained by the system.

This prediction for the qSS is similar to the one proposed in 2011 [32] for the HMF system and is limited to specific states, known as virial states, as discussed in [24] and [33]. Outside of these states, the magnetization evolves over time, leading to significant discrepancies between theoretical predictions and simulations. As highlighted in [32], in the case presented in Fig. 1, there is an observed increase in magnetization during the system's relaxation. Additionally, while the energy should be preserved as a Casimir invariant in the Vlasov dynamics, when magnetization evolves over time, the local mixing process can also result in a decrease in the total energy of the system, as we will demonstrate below.

To better illustrate this phenomenon, we consider an initial scenario where all HMF particles are located at two distinct points in phase space, $(\theta, p) = (0, \pm p_0)$. In this configuration, the total energy of the system is $U_0 = Np_0^2/2$, with an initial magnetization of $m_0 = 1$. The resulting coarse-grained distribution function after the particles spread over the isoenergy surface is $\bar{f}_0(\epsilon) = g_0(\epsilon)^{-1}$ such that the new total energy is found to be:

$$\frac{U}{U_0} = 1 - \frac{p_0^2}{4} \left(1 - \frac{E[\kappa_0^{-1}]}{K[\kappa_0^{-1}]} \right)^2. \quad (7)$$

where $E(x)$ is the complete elliptic integral of the second kind, for simplicity we are considering the real parts of both $E(x)$ and $K(x)$. Clearly the process of mixing resulted in lower total energy of the system.

The aim of this work is to propose that, as magnetization evolves during the mixing process, the released energy is carried away by particles excited through parametric resonances, resulting in evaporative cooling of the core region. The final qSS is then determined iteratively as a map, where time corresponds to an index i , with $i = 0$ representing the initial state. The magnetization in iteration $i + 1$ associated with the coarse-grained dis-

tribution at i can be computed as:

$$m_{i+1} = \iint d\theta dp \bar{f}_i[\varepsilon_i(\theta, p)] \cos \theta. \quad (8)$$

Writing,

$$\bar{f}_i[\varepsilon_i(\theta, p)] = \int d\epsilon \bar{f}_i(\epsilon) \delta[\varepsilon_i(\theta, p) - \epsilon]. \quad (9)$$

and substituting this in Eq. (8) and exchanging the order of integration, we obtain:

$$m_{i+1} = 4 \begin{cases} \int d\epsilon \frac{m_i[2E(\kappa_i) - K(\kappa_i)]}{\sqrt{|m_i|^3}} \bar{f}_i(\epsilon) & \text{if } \kappa_i \leq 1 \\ \int d\epsilon \frac{m_i[(1-2\kappa_i)K(\kappa_i^{-1}) + 2\kappa_i E(\kappa_i^{-1})]}{\sqrt{\kappa_i|m_i|^3}} \bar{f}_i(\epsilon) & \text{if } \kappa_i > 1 \end{cases} \quad (10)$$

where the lower limit of the integral is $1 - |m_i|$. The expressions for $\bar{f}_i(\epsilon)$ and g_i are identical to those of $\bar{f}_0(\epsilon)$ and g_0 , as given in Eqs. 4 and 6 with the index 0 replaced by i . The same for κ_i and ε_i that corresponds to κ_0 and ε_0 with the index 0 replaced by i . The updated magnetization m_{i+1} , will change the isoenergy trajectories, so that the particles that were distributed according to the coarse-grained distribution $\bar{f}_i(\epsilon)$ will now redistribute over the new isoenergy contours defined by $\varepsilon_{i+1}(\theta, p)$, resulting in a new coarse-grained distribution:

$$\bar{f}_{i+1}(\epsilon) = \frac{\iint d\theta dp \bar{f}_i[\varepsilon_i(\theta, p)] \delta[\varepsilon_{i+1}(\theta, p) - \epsilon]}{\iint d\theta dp \delta[\varepsilon_{i+1}(\theta, p) - \epsilon]}. \quad (11)$$

Using the properties of the delta function, the integral over momentum can be performed explicitly resulting in:

$$\bar{f}_{i+1}(\epsilon) = \frac{\int d\theta \frac{\bar{f}_i(\epsilon - \delta m_i \cos \theta)}{\sqrt{2(\epsilon - 1 + m_{i+1} \cos \theta)}}}{g_{i+1}(\epsilon)}, \quad (12)$$

where $\delta m_i = m_i - m_{i+1}$. The evolution described by the map Eqs. (10) and (12) terminates when m_∞ reaches a fixed point or a limit cycle. In all cases studied the ferromagnetic state always corresponds to a fixed point of the map, while paramagnetic state is found to be either a fixed point with $m_\infty = 0$ or a limit cycle with small oscillations around $m_\infty = 0$. In the latter case to define the magnetization of the qSS we will take the average over the limit cycle.

To compensate for the cooling of the core produced by the mixing process we, therefore, introduce a halo region which extends from the maximum energy of the core particles, which we shall denote as the Fermi energy ϵ_F , up to the halo energy ϵ_h . The maximum energy of evaporating particles ϵ_h can be calculated using the canonical perturbation theory [2, 27]. The population of particles in the halo region is assumed to be uniform in the phase space, consistent with the Landau damping mechanism that progressively decreases the oscillation of the mean-field potential leading to the final qSS. We thus propose

a local mixing core-halo (LMCH) ansatz for the particle distribution in the qSS:

$$\bar{f}_{qSS}(\epsilon) = \bar{f}_\infty(\epsilon)\Theta(\epsilon_F - \epsilon) + \chi\Theta(\epsilon - \epsilon_F)\Theta(\epsilon_h - \epsilon). \quad (13)$$

The core region, described by the map Eqs. (10) and (12), is bounded by the Fermi energy. Above ϵ_F the particles are uniformly distributed up to ϵ_h . The values of ϵ_F and the phase space density of the halo particles χ are calculated self-consistently to preserve the total energy of the system and the norm of the distribution function. The marginal distributions can be obtained as follows:

$$\begin{cases} n_i(\theta) = \int dp \bar{f}_i[\varepsilon_i(\theta, p)] \\ n_i(p) = \int d\theta \bar{f}_i[\varepsilon_i(\theta, p)]. \end{cases} \quad (14)$$

An example of the marginal distribution functions calculated using the present theory are shown in the Fig. 1. As can be seen from the figure, there is an excellent agreement with the results of MD simulations, while LB and CH theories predicts a qualitatively incorrect form of the distribution function.

The HMF model is known to exhibit a phase transition between ordered and disordered phases [1]. The transition has been investigated using MD simulations and LB and CH theories. It was shown that LB incorrectly predicts the order of the phase transition even for the simplest one level water-bag initial distribution of particles [19, 34]. Very little is known about the non-equilibrium phase transitions of continuous initial particle distributions. The non-linear stability analysis based on Vlasov equation can be used to predict that for a class of concave distribution functions an initial paramagnetic state will become unstable below some energy threshold [35]. However, nothing is known analytically about the qSS to which the system will relax or even if the qSS will remain paramagnetic or become magnetized. Nothing is known about the relaxation of initially convex (population inverted) distributions.

To demonstrate the broad applicability of the LMCH theory, we will examine the out-of-equilibrium phase transitions in the HMF model starting from an initial paramagnetic state. We consider three distinct initial distributions: water-bag, concave, and convex. In analogy with the equilibrium order-disorder phase transitions, we will define the transition to be first order if the magnetization histogram in the transition region exhibits three peaks, corresponding to the ‘‘coexistence’’ of qSS states with $\pm m$ and 0, magnetizations, see Figs. 2, 3, and 4. The histograms are constructed by tabulating the values of magnetization of the final qSS, m_{qSS} , to which the system will evolve starting from an initial state drawn from the probability distribution $f_0(p, \theta)$. In simulations we have used $N = 2 \times 10^5$ particles. The standard deviations and histogram were calculated using 10^4 random realizations of the initial conditions. We see

that for all the distributions studied, phase transition are found to be of first order.

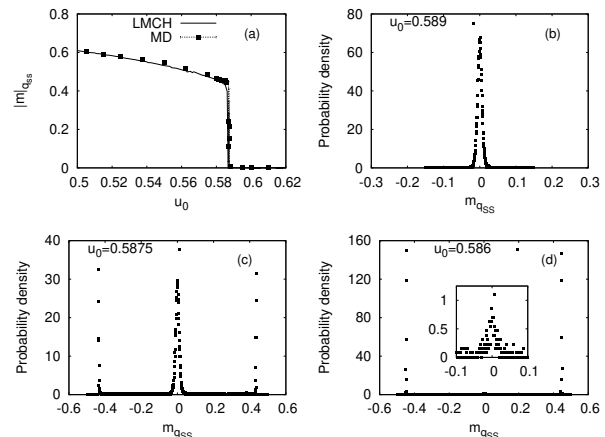


FIG. 2. The magnetization of the final qSS starting from initial water-bag particle distribution $f_0(\theta, p) = \frac{1}{4\pi p_0}\Theta(p_0 - |p|)$, as a function of the initial energy per particle u_0 . Panel (a) shows the modulus of magnetization $|m|_{qSS}$ in the final qSS, as a function of the initial energy. The solid lines represent theoretical predictions of LMCH theory, while symbols depict results of molecular dynamics (MD) simulations. Panels (b), (c), and (d) show histograms of magnetization for various u_0 after 10^4 different random realizations. The transition region is characterized by the coexistence of three peaks indicating a first order phase transition. The subplot in panel (d) is included to adjust the scale of the plot. Away from the transition region, the error bar size is comparable to the size of the data points.

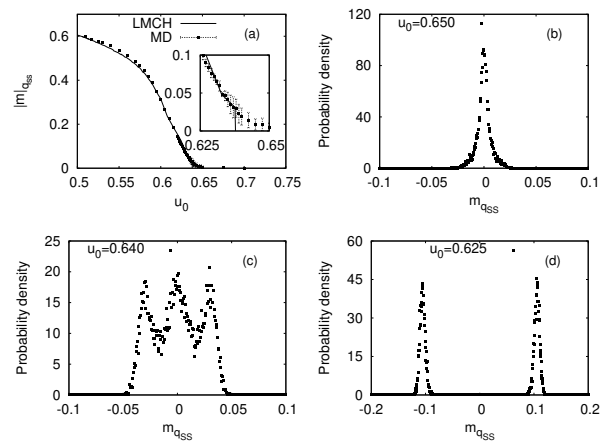


FIG. 3. Same as in Fig. 2 but with initial concave particle distribution $f_0(\theta, p) = \frac{3}{8\pi p_0} \left[1 - \left(\frac{p}{p_0} \right)^2 \right] \Theta(p_0 - |p|)$.

For the two initial distributions presented in Figs. 2 and 3 one can use the non-linear stability analysis [35–39] to predicts that the critical energy at which initial water-bag and (concave) parabolic distributions will become

unstable: $u_0^* = 7/12$ and $u_0^* = 13/20$, respectively. These values are in agreement with the appearance of the paramagnetic peak when energy per particle exceeds $u_0 > u_0^*$ and are in accordance with the prediction of LMCH theory. Thus, the theory presented in this Letter agrees with the predictions of the non-linear stability analysis. However, in addition to the instability threshold, it predicts that the initial paramagnetic state will evolve to a ferromagnetic qSS through a first order phase transition. The LMCH theory also allows us to very accurately predict the resulting magnetization of the final qSS, see Figs. 2a, 3a, and 4a. In the case of convex (population inverted) initial distributions the non-linear stability theory can not be applied [35] and nothing is known about phase transitions of such initial states. In Fig. 4, we show the predictions of LMCH applied to initial population inverted parabolic distribution of particle velocities. The simulations show that the transition region characterizing convex distributions is extremely complex, with the probability measure of magnetized states described by a very broad distribution of magnetizations, see Fig. 4c. This is also reflected in the huge standard deviations that appear in the transition region of Fig. 4a. Nevertheless, we see a “coexistence” of three dominant peaks in the histogram, which allow us to denote the phase transition as “first order”. The critical energy u_0^* at which a paramagnetic $m = 0$ peak first appears agrees with the location of the first order phase transition predicted by the theory, see Fig. 4a.

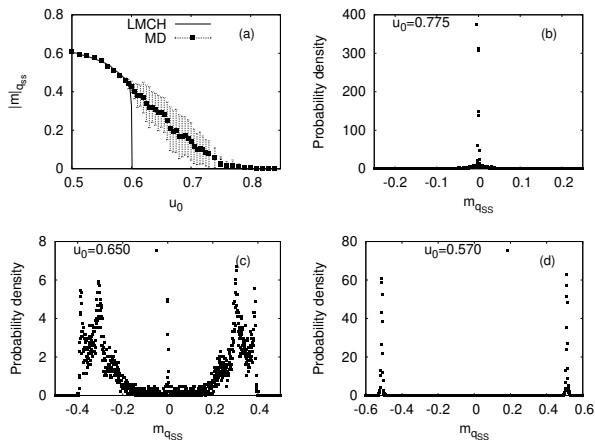


FIG. 4. Same as in Fig. 2 but with initial convex (population inverted) particle distribution $f_0(\theta, p) = \frac{3}{4\pi p_0} \left(\frac{p}{p_0}\right)^2 \Theta(p_0 - |p|)$. The transition region is characterized by huge fluctuations of the order parameter, reflected by very large standard deviations in magnetization of the final qSS.

In summary, the presented theory enhances our understanding of collisionless relaxation in long-range interaction systems and integrates existing qSS predictions from LB’s 1967 work to the present. Despite broken ergodicity, these systems exhibit local mixing along isoenergy

curves. Our approach allows for quantitative predictions of qSS distribution functions across arbitrary initial conditions and addresses non-equilibrium phase transitions in long-range systems. We also clarify the nature of the nonequilibrium phase transition in the HMF system. Notably, before the $m = 0$ peak disappears, a stable magnetized state persists, leading to bistability. This phenomenon, while reminiscent of short-range interactions, is fundamentally different because the LR system remains in either the $m = 0$ or $m \neq 0$ state after reaching a specific initial condition. This represents the first clear demonstration of bistability for both water-bag and other continuous distributions. Additionally, our approach predicts transitions to distributions unsupported by Vlasov equation stability theories. Future work will explore applications of this theory to self-gravitating systems and magnetically confined plasmas.

* levin@if.ufrgs.br

- [1] A. Campa, T. Dauxois and S. Ruffo, Phys. Rep. **480**, 57 (2009).
- [2] Y. Levin, R. Pakter, F. B. Rizzato, T. N. Teles, and F. P. C. Benetti, Phys. Rep. 535, 1 (2013).
- [3] M. Kac, G. E. Uhlenbeck, and P. C. Hemmer, J. Math. Phys. **4**, 216 (1963).
- [4] J. Barré, D. Mukamel, and S. Ruffo, Phys. Rev. Lett. **87**, 030601 (2001).
- [5] L. Chakhmakhchyan, TN Teles, S Ruffo, Journal of Statistical Mechanics: Theory and Experiment, Volume 2017, June 2017.
- [6] W. Thirring, Z. Phys. 235, 339 (1970);
- [7] Tarcísio N. Teles, Shamik Gupta, Pierfrancesco Di Cintio, and Lapo Casetti Phys. Rev. E 92, 020101(R)
- [8] T. Padmanabhan, Phys. Rep. **188**, 285 (1990).
- [9] H. Touchette, Phys. Rep. **478**, 1 (2009).
- [10] David Mukamel, AIP Conf. Proc. 11 January 2008; 970 (1): 22–38
- [11] Y. Levin, R. Pakter, and T. N. Teles, Phys. Rev. Lett. **100**, 040604 (2008).
- [12] F. Bouchet and A. Venaille, Phys. Rep. **515**, 227 (2012).
- [13] P. H. Chavanis, Phys. Rev. Lett. **84**, 5512 (2000).
- [14] Nicolò Defenu, Tobias Donner, Tommaso Macrì, Guido Pagano, Stefano Ruffo et al. Rev.Mod.Phys. 95 (2023) 3, 035002
- [15] S. Slama, S. Bux, G. Krenz, C. Zimmermann, and P. Courteille, Phys. Rev. Lett. **98**, 053603 (2007).
- [16] W. Braun and K. Hepp, Comm. Math. Phys. **56**, 101 (1977).
- [17] D. Lynden-Bell, Mon. Not. R. Astron. Soc. **136**, 101 (1967).
- [18] T. M. Rocha Filho, A. Figueiredo and M. A. Amato, Phys. Rev. Lett. 95 (2005) 190601.
- [19] R. Pakter, and Y. Levin, Phys. Rev. Lett. **106**, 200603 (2011).
- [20] T. N. Teles, Fernanda P. da C. Benetti, R. Pakter, and Y. Levin, Phys. Rev. Lett. 109, 230601 (2012).
- [21] F. P. C. Benetti, A. C. Ribeiro-Teixeira, R. Pakter, and Y. Levin, Phys. Rev. Lett. 113, 100602 (2014).

- [22] Alessandro Santini et al J. Stat. Mech. (2022) 013210
- [23] Ewart R.J, Nastac ML, Schekochihin AA. Journal of Plasma Physics. 2023;89(5):905890516.
- [24] F. P. da C. Benetti, T. N. Teles, R. Pakter, and Y. Levin, Phys. Rev. Lett. **108**, 140601 (2012).
- [25] Lecar, M. ,International Astronomical Union: Paris, France, 1966; Volume 25, p. 46.
- [26] Hohl, F.; Feix, M.R. Astrophys. J. 1967, 147, 1164.
- [27] Robert L. Gluckstern Phys. Rev. Lett. 73, 1247.
- [28] Tarcísio N. Teles, Calvin A. F. Farias, Renato Pakter and Yan Levin, Entropy 25, 1379, (2023).
- [29] M. Antoni and S. Ruffo, Phys. Rev. E **52**, 2361 (1995).
- [30] T.N. Teles, R. Pakter, Y. Levin, Applied Phys. Lett. 95, 173501 (2009).
- [31] X. Leoncini, T. Van Den Berg, and D. Fanelli, Europhys. Lett. 86, 20002 (2009).
- [32] P. de Buyl, D. Mukamel, and S. Ruffo, Phys. Rev. E **84**, 061151 (2011).
- [33] A. C. Ribeiro-Teixeira, F. P. C. Benetti, R. Pakter, and Y. Levin, Phys. Rev. E **89**, 022130 (2014).
- [34] A. Antoniazzi, F. Califano, D. Fanelli, and S. Ruffo, Phys. Rev. Lett. **98**. 150602 (2007).
- [35] Y. Y. Yamaguchi, J. Barré, F. Bouchet, T. Dauxois, and S. Ruffo, Phys. A Stat. Mech. Its Appl. 337, **36** (2004).
- [36] J. D. Crawford, Phys. Rev. Lett. 73, 656 (1994).
- [37] S. Ogawa et al., Phys. Rev. E 89, 052114 (2014).
- [38] D. D. Holm, J. E. Marsden, T. Ratiu, A. Weinstein, Phys. Rep. 123, 1 (1985)
- [39] V. I. Arnold, Izv. Vyssh. Uchebn. Zaved. Matematika 54 (5) 3-5 (1966); Engl . transl.: Am. Math. Soc. Trans.

